Modelling masonry arch bridges using commercial finite element software

T.E. Ford, C.E. Augarde and S.S. Tuxford
School of Engineering,
University of Durham,
South Road, Durham, UK.

Paper to be presented at the 9th International Conference on Civil and Structural Engineering Computing, Egmond aan Zee, The Netherlands, 2-4 September 2003

Abstract

Numerical models of masonry arch bridges are required for accurate determination of ultimate failure loads. Finite element analysis (FEA) has been surprisingly under-used in this area perhaps because the main features of masonry behaviour, namely strongly non-linear loss of stiffness through cracking and failure of an arch by the formation of a mechanism, are hard to model using conventional continuum elements, familiar to industrial users. This paper describes models of masonry arch bridges built within a basic FEA package, basing numerical results on field data from tests to destruction on arch bridges.

Keywords: masonry arch bridges, finite element modelling, crack modelling

1 Introduction

Masonry arch bridges have been used for at least 4000 years. In many countries, the UK in particular, a large number of old masonry arch bridges still form part of the highway and railway networks. Due to the over-conservative design methods used in earlier times, these bridges are usually able to carry the ever-increasing live loads from modern day traffic without risk of collapse. They have also proved themselves to have been an extremely durable structural form and are generally considered aesthetically pleasing.

In recent years, considerable effort has been put into gaining a greater understanding of the behaviour of masonry arch bridges to improve efficiency when assessing a bridge's ultimate strength. Many techniques used for assessment have been recognised as being highly conservative, i.e. predicting collapse loads far lower than predicted by experience. At present, finite element analysis is usually considered too impractical for use in masonry arch assessment by civil engineering consultants, as it often requires input parameters that cannot easily be determined. This paper describes a new finite element model of a masonry arch bridge built within a conventional commercial FEA package. The model is "tuned" against the

widely available data from testing by the Transport Research Laboratory (TRL) in the 1980's [1] and provides a useful indication of the value of FEA for assessment engineers with access to basic FEA software.

2 Assessment methods

The assessment methods used in industry for determination of the ultimate strength of a masonry arch bridge are reviewed in Hughes and Blackler [2]. In the majority of methods, the strength of the bridge is taken as equivalent to the strength of the arch barrel alone. The effects of spandrel walls, wing walls, fill and parapets are usually ignored. The "MEXE" procedure is probably the most commonly used method in industry in the UK. It is semi-empirical but (believed) to be based on an elastic analysis by Pippard who modelled the arch barrel as linear elastic, segmental in shape, pinned at its supports and carrying a central point load. The maximum load determined by this procedure is modified by a number of (in some cases) highly subjective parameters. The MEXE method is known to be over-conservative but is quick and easy to use.

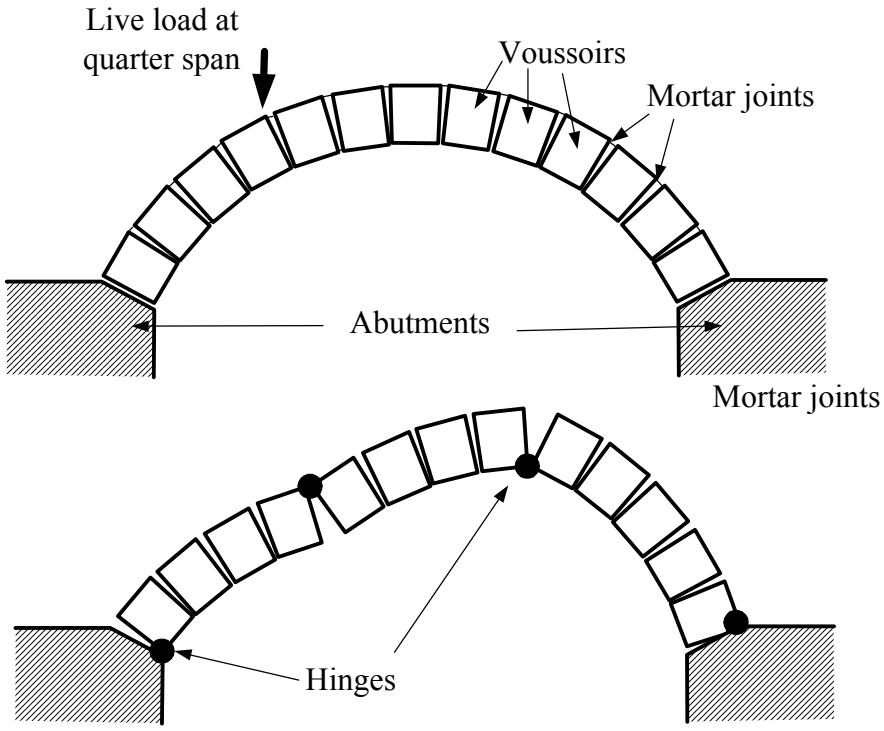

Figure 1: Idealisation of arch barrel and mechanism failure.

The Mechanism Method is a more rational approach where the arch barrel is assumed to collapse by the formation of a four-hinge mechanism (as shown in Figure 1). Simple equilibrium calculations lead to the value of failure load (balanced by the self-weight of the arch barrel) for a given mechanism. This procedure is repeated with different mechanisms until a minimum load is found. For a plain arch barrel and a point load the worst load position is usually found to lie close to quarter-span (as shown in Figure 1).

The Mechanism Method has recently been developed into modern software where the user does not have to iterate to find the worst-case mechanism. Examples currently available are the spreadsheet developed at Cardiff University [3] and the commercial software Archie-M [4]. The Mechanism Method is attractive not just because it is more rigorous than the MEXE method but because formation of mechanisms at failure have been witnessed in the relatively few large scale tests carried out on masonry arch bridges [1]. Modern forms of the Mechanism Method can also take account of the fill overlying the arch barrel, which serves to increase the bridge's strength, by its self-weight, and by the passive resistance mobilised by parts of the mechanism moving upwards during failure.

Other assessment methods are described by Hughes & Blackler [2] but none have proved as popular as the two described above. Gilbert and Melbourne [5] have for a number of years developed methods based on classical plasticity theory, where forces between voussoirs in an arch barrel are the variables in a linear programming problem. This method has also recently been developed into user-friendly software in conjunction with the UK rail industry [6].

2.1 The use of finite element methods

Perhaps surprisingly, given its omnipotence in other areas of structural analysis, relatively little research has been published on the feasibility of FEA for masonry arch bridge assessment. The reasons for this could be:

- The existing methods are satisfactory.
- Masonry arch bridges have considerable reserves of strength and stability.
- To date FE programs available to consulting engineers have not had the power to model a masonry arch bridge in detail.

Towler [7] and Crisfield [8] appear to have been the first researchers to experiment with FEA in this area, in the 1980's. Both went on to simulate the effect of fill using, in one case, horizontal non-linear springs to model passive pressure from the soil [8]. In these works and later research [9] macroscopic modelling is used where voussoirs (see Fig. 1) are not modelled individually but a single constitutive formulation is used to model masonry (i.e. the voussoirs and the mortar joints combined), a so-called "smeared crack technique" [9] or macro-modelling. While these pieces of research and others (e.g. [10]) use FEA they have not transferred widely to industry perhaps because they were developed outside the confines of commercial FEA packages.

More recently, however, Ng et al. [11] describes analysis of masonry arch bridges using general-purpose FEA software (LUSAS) and reports close agreement between predictions from FEA and the results of the full-scale tests carried out under the TRL program [1]. Thavalingham et al. [12] compares different approaches to computational modelling of masonry arches, including discrete element modelling and non-linear FEA and conclude that the latter is preferable due to ease of use and issues such as convergence. Aspects of both of these studies appear in the models described below although a slightly different approach is taken to the last of the references described above in that it is based fully within the confines of an existing (and by no means complex) FEA package.

3 Development of a finite element model using Strand7

The FEA package used in this research is "Strand7", developed by G + D Computing. This is a general purpose FEA package used in the aero industry for stress analysis which is becoming more popular in general structural analysis. It is similar to other (perhaps better known) packages such as LUSAS and ABAQUS but contains many fewer material models and element types than either.

A two-dimensional plane strain model of an arch barrel is developed here. The assumption of plane strain implies a straight (rather than skew) span and a bridge of a comparable width in comparison to span (a reasonable assumption for most UK road and rail bridges that one would wish to assess). A single span is modelled, this being the first step before progressing onto a multi-span structure.

As described above, the most common mode of failure for a masonry arch bridge is the formation of a mechanism. Hinges are formed in the arch barrel due to cracking of voussoirs, the mortar joints or bond failure between the two. Allowing only mechanism failure in this model is not a major drawback, since it reduces the complexity considerably. Clearly, masonry arches do fail by other means, such as snap-through or by compressive failure, but mechanism collapse appears dominant [1], unless the bridge is in a particularly poor condition. Since failure starts with cracking it therefore appears that fracture modelling is necessary. Whilst fracture could be modelled it would turn the approach towards research rather than practice. In practice a hinge can form anywhere in the arch barrel, however in this model planes of weakness are built into the arch barrel at discrete locations. These correspond to the areas where cracking is expected from previous field experience and the results of typical Mechanism Method analyses.

Figure 2 shows a finite element model of the segmental arch barrel of Strathmashie Bridge. (This bridge was one of a group of redundant structures tested to destruction by the Transport Research Laboratory in the 1980's. Some dimensions

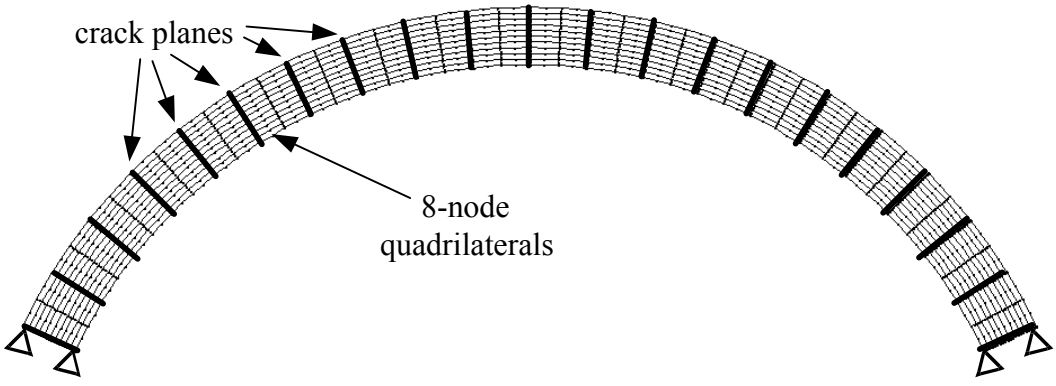

Figure 2: General arrangement of finite element model of an arch barrel

and failure loads for bridges in this group are given in Appendix 1). As in previous research discussed above, macro- rather than micro- modelling is used. Apart from the additional computational complexity of a micro-model of a masonry arch bridge many more material parameters must be known, such as, the coefficient of friction

between voussoirs or the shear strength of each mortar joint. These material properties are difficult to obtain and therefore make micro-modelling an impractical method of analysing a bridge.

The barrel voussoirs and mortar joints are modelled using conventional eight-noded quadrilateral elements which are laid out regularly and do not follow a particular pattern of voussoirs. Radial planes of weakness ("crack planes") are inserted into the barrel at pre-determined intervals. Each crack plane subtends an angle of 0.1^{o} in this model. A close-up view of a crack plane is shown in Figure 3. To allow the formation of a hinge, nodes on the sides of the crack plane are connected by point contact elements. These elements behave linear elastically in compression and up to a cut-off tension, T that is user-defined (as is the stiffness). Once tension reaches T the stiffness drops to zero thus modelling the loss of all tensile stiffness across an open crack in masonry.

In addition to assuming that masonry has zero tensile strength, the Mechanism Method (and more advanced procedures, initially at least [5]) also assumes that sliding failure cannot occur between voussoirs. Initial experiments in this study with crack planes using point contact beams alone were not successful and analyses failed to converge. The reason for this behaviour is sliding between voussoirs along the crack planes, leading to an unrealistic failure mode similar to snap-through. To prevent this occurring shear panel elements are also included in the crack planes (see Figure 3). These are linear elastic four-noded quadrilateral plate elements that carry in-plane shear only.

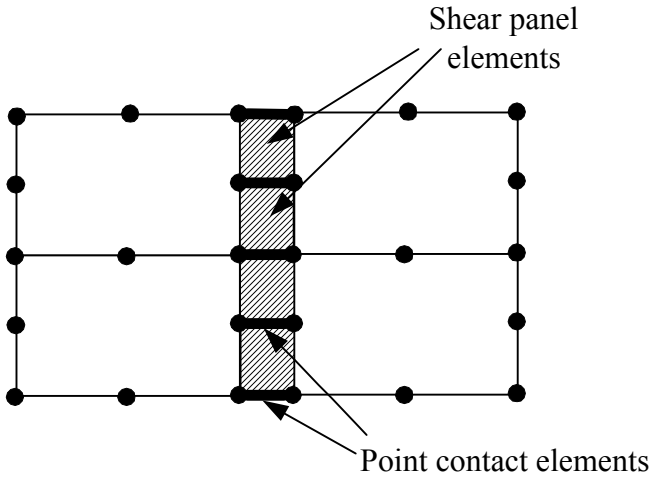

Figure 3: Close-up of a crack plane

The behaviour of crack planes in the analysis of an arch barrel produces a hinge as required. Figure 4 shows a portion of the Strathmashie arch barrel as it is loaded at its quarter-point for two load increments between which a hinge forms. Non-dimensional contours of von Mises stress are shown to illustrate the changes in stresses before and after hinge formation (darker areas are low stress). In Figure 4a, the tensions in the point contact beams are all less than T and the continuum elements either side of the crack transmit stresses across the crack plane. Following

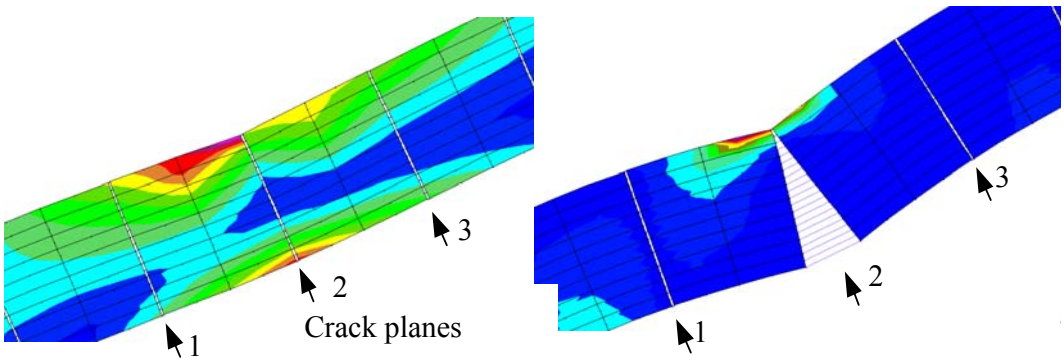

(a) Before hinge (b) After hinge

Figure 4: Crack plane before and after hinge formation

hinge formation, in Figure 4b, a majority of the point contact elements have dropped to zero stiffness and continuum elements either side of the plane have unloaded. High stress gradients (which are circumferentially compressive) are apparent at the top of the crack plane where the hinge pivots. The main unknown that determines the point at which a hinge forms is the value of T in the point contact elements. It follows that if mechanism formation is the mode of failure, then. T must control the failure load for the arch.

Non-linear material behaviour is also defined for the continuum elements modelling the voussoirs, although for simplicity this is not elasto-plastic but nonlinear elastic. A maximum stress criterion is used to define when behaviour changes from linear elastic to recoverable yield, and values can be different in compression and tension. Elasto-plastic macro-modelling of masonry is possible and has been carried out by many researchers, but usually for different problems (e.g. [13, 14]). In the analysis of masonry arch bridges we are primarily concerned with failure loads rather than deformations and so avoiding the inclusion of potential plasticity in the model (and the difficulties that can bring in solution) appears reasonable given the initial goals of this work, stated above.

4 Analysis procedure

Formation of a mechanism in a masonry arch barrel implies complete loss of stiffness at failure. Since the analyses described here are load- rather than displacement-controlled (i.e. we wish to determine the collapse load of an arch) it is difficult if not impossible to reach the point of collapse with conventional finite element procedures. Other ways are needed to assess when failure is due to occur.

Several ways of defining failure of an arch in these analyses are possible. A visual inspection of the finite element results model can be carried out, and failure deemed to occur when the fourth (and final) hinge appears to begin forming. A predefined displacement can also be used to define failure, although this is difficult to carry over between bridges, although a relation linking span, rise and arch thickness could be developed for this purpose. Non-linearities are present in the model due to the point contact elements in the crack planes and the material of the

main barrel elements. A modified Newton-Raphson procedure is used to deal with these non-linearities in Strand7. An alternative way of defining failure is to link it to non-convergence of the solution. This occurs when the structure stiffness matrix has become singular and hence no unique solution exists. However, the user can control the solver behaviour to a small degree by defining when to stop iterating within a particular load stage. In Strand7, two norms are used to determine convergence. The displacement norm at increment i is defined as

$$\frac{\|\Delta \mathbf{d}_i\|}{\|\mathbf{d}\|} \tag{1}$$

where $\Delta \mathbf{d}_i$ and $\mathbf{d}$ are incremental and total displacement vectors respectively. The residual force norm is defined as:

$$\frac{\|\mathbf{R}_i\|}{\|\mathbf{P}_0\|} \tag{2}$$

where $\mathbf{R}_i$ is the residual force vector at increment i and $\mathbf{P}_0$ is the residual force vector at the first increment of the current load stage. A load stage is deemed to have converged if both

$$\frac{\|\Delta \mathbf{d}_i\|}{\|\mathbf{d}\|} < \varepsilon_d \qquad \textit{and} \qquad \frac{\|\mathbf{R}_i\|}{\|\mathbf{P}_0\|} < \varepsilon_\gamma \tag{3}$$

where ε_d and ε_γ are tolerances that can be adjusted by the user. If stiffness becomes very small, indicating imminent mechanism formation in an arch model, then the displacement norm check may never be reached, or the solution will certainly exceed the maximum iteration count allowed. In an ideal case we would like to be able to set these norms so that the only the final load step in an analysis failed to converge. In the analyses described below, the values of these norms are varied to note their effect on the behaviour of the models and hence to provide guidance for other users.

5 Modelling failure of arch barrels

The results from models of three bridges tested under the TRL programme (details in Appendix 1) are given here. The results give suitable values of the tension cut-off point T for the crack planes. The results also indicate, unfortunately, that there is little apparent pattern to follow by a user for the controlling norms to avoid non-convergence to a solution before the final load increment. As stated above, T is likely to be the most important parameter in determining the collapse load for an arch model. Knowledge of its value *a priori* is necessary if this type of model is to

be used on bridges under assessment (rather than comparing to the test bridge data that are used here) and guidance from the three test bridges here is undoubtedly useful. In all analyses, gravity loading is applied in an initial load stage before application of live point loading in a number of increments.

5.1 Strathmashie Bridge

The material properties used in this model are given in Table 1

Main voussoir elements		**Shear panels**		**Point contact elements**	
Young's Modulus	5 GPa	Shear modulus	80 GPa	Initial axial Stiffness	200 GN/m
Poisson's ratio	0.49	Poisson's ratio	0.2	Maximum Tension	6.2 MN
Density	2200 kg/m^3				

Table 1: Material properties used for Strathmashie Bridge model

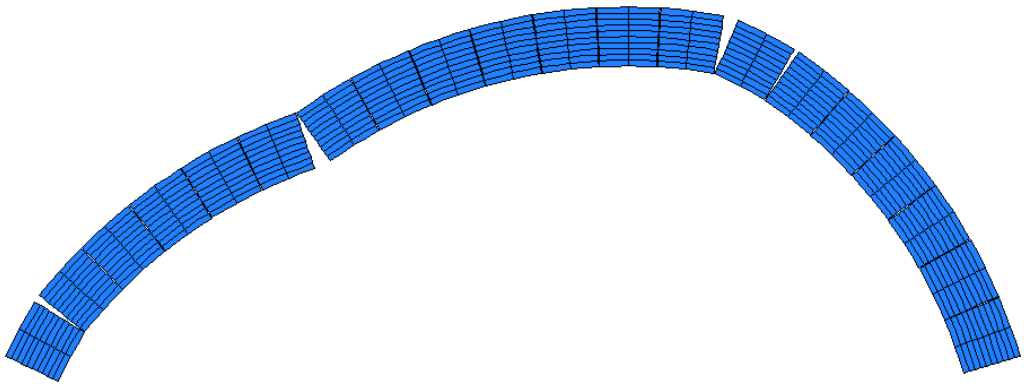

Figure 5: Strathmashie bridge barrel at failure load

The finite element mesh for this model is shown in Figure 2 and has 1720 nodes, 400 eight-node quadrilateral elements, 420 shear panel elements and 441 point contact elements. After some experimentation the value of T found to give an equivalent failure load to that in Appendix 1 was 6.2 MN. While the use of the non-linear elastic material model for the voussoirs changed the displacements of the arch during loading it did not have any effect on the failure load for the same value of T. The deformed shape of the arch at the correct failure load (to an increased scale) is shown in Figure 5. Hinges can be seen beneath the point load (on the left hand side) at or close to the abutments and close to the opposite quarter span. This arrangement of hinges corresponds well to the results of a Mechanism Method analysis of this arch.

The norms used to achieve the final result with this model were $\varepsilon_d = 0.01$ and $\varepsilon_\gamma = 0.2$. These are considerably higher than the norms set as default in non-linear

solvers of this nature ($\varepsilon_d = 0.0001$ and $\varepsilon_\gamma = 0.001$ are typical values). They demonstrate the instability of the model perhaps dictated by the sharp change in stiffness of the point contact elements in the crack planes.

5.2 Bridgemill bridge

The original Bridgemill Bridge was parabolic in shape but was very shallow. Therefore a segmental shaped mesh was used in this study, for ease of generation. The mesh is shown in Figure 6 and has a similar number of nodes and elements as the Strathmashie model. Once again, twenty-one crack planes subtending 0.1° each were placed in the arch barrel and the same properties used for the voussoir

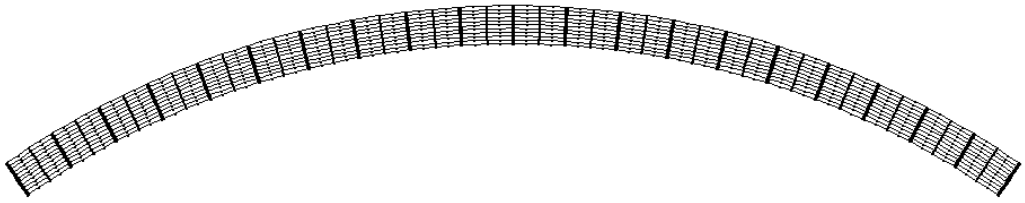

Figure 6: Bridgemill barrel model

elements, the shear panels and the point contact elements. The norms used for Strathmashie were used in Bridgemill, to investigate how the convergence of a solve related to this bridge model.

As with Strathmashie, the presence of the non-linear material model for the voussoirs served only to change displacements and had no effect on the failure load. This is to be expected in an analysis without considering the effects of geometrical non-linearity. Using the *T* value from Strathmashie resulted in a failure load for this bridge 21% higher than that found in reality (See Appendix 1). By reducing *T* to 3.7MN agreement was reached. Keeping the norm tolerances the same as used in the Strathmashie model resulted in all of the Bridgemill solves converging, even when four hinges were formed. Therefore, norms were adjusted, after some experimentation to $\varepsilon_d = 0.02$ and $\varepsilon_\gamma = 0.001$. This however, produced irregular convergence properties. In a ten-step analysis (i.e. the failure load applied in ten equal increments) stages 2, 6 & 7 failed to converge. This could be due to the formation of hinges prior to the final mechanism failure but it indicates that it is difficult to provide definite rules on these norm levels for these models.

5.3 Barlae Bridge

The mesh for Barlae Bridge was the same in all respects, except geometry, to the previous two bridge models. (The geometry of Barlae Bridge was between the two extremes of Strathmashie and Bridgemill; both in terms of span-to-rise ratio and the ring thickness to span ratio). Surprisingly, using the value of *T* from the Strathmashie model resulted in a predicted failure load of 8% above that found in

reality indicating that for accurate modelling of this bridge T should be slightly lower than 6.2MN.

5.4 Comparison of barrel analyses

The results from the three bridge models give a strong indication of the levels of parameter T required for accurate modelling of arch barrels. The values appear high given the failure loads but a simple calculation shows them to be reasonable. The loads in the point contact elements are of the same order of magnitude as those consistent with the maximum longitudinal stresses in a simply-supported beam of the same span and thickness as the arch under this loading applied at the centre. What is less clear is how to devise a rule to determine T for other arch models.

	T (MN)	Span to rise ratio	Span to thickness ratio
Strathmashie	6.2	3.1	16
Bridgemill	3.8	6.4	26
Barlae	5.7	5.8	22

Table 2: comparison of bridge barrel parameters

Table 2 shows T for these bridge barrel models together with two dimensionless ratios that describe the bridge geometry. In both cases the level of T is inversely proportional to the ratio. For the span-rise ratio this is perhaps understandable. Bridgemill is the flattest of the arches by this measure and is therefore likely to be least circumferentially precompressed by initial self-weight than the other bridge barrels. The relationship between T and the span-thickness ratio is harder to explain.

6 Modelling arches with fill

6.1 Finite element considerations

Determining bridge failure loads by modelling arch barrels alone is clearly conservative, despite the fact that such analysis is accepted and used widely in the UK. The fill over an arch will always increase the failure load of the bridge providing it is uniform and the effects of water are ignored. The next stage in this investigation is the inclusion of fill into models of the three bridges described above.

Fill over arch barrels can vary in practice from clean well-graded granular material to compacted clay. The role of the fill is twofold. Firstly, the presence of the fill distributes concentrated loads on the running surface over the bridge. Secondly, its self-weight increases stability by inducing greater initial compression in the arch prior to live loading. Both of these characteristics of fill can be modelled using linear elasticity. Using linear elasticity for modelling the behaviour of soil is

acknowledged as being crude but is reasonable to avoid over complexity in a problem where deformations are of less concern than failure loads.

Before adding fill to the finite element mesh, it is necessary to consider the nature of the interface between the fill and the arch barrel. The behaviour of the interface must vary between two extremes, full fixity due to friction, and to a lesser extent adhesion, and fully smooth. Quite where the real behaviour sits in this spectrum is impossible to determine with any accuracy for a real arch bridge.

The first attempt to model the interface is shown in Figure 7. The interface is modelled in a similar way to the crack planes in the arch barrel. Nodes on the extrados of the arch barrel are connected to continuum elements (eight-noded quadrilaterals) using point contact elements, and shear stiffness of the interface is provided by shear panel elements. The arch barrel elements are graded to fit with the refinement in the fill mesh. Initially point contact elements with a zero-tension cut-off (i.e. $T = 0$) were used to allow for possible separation between the barrel and the fill, however these were later changed to have a positive tension cut-off as separation became the dominant mode of behaviour, even at very low imposed loads, not in line with empirical evidence.

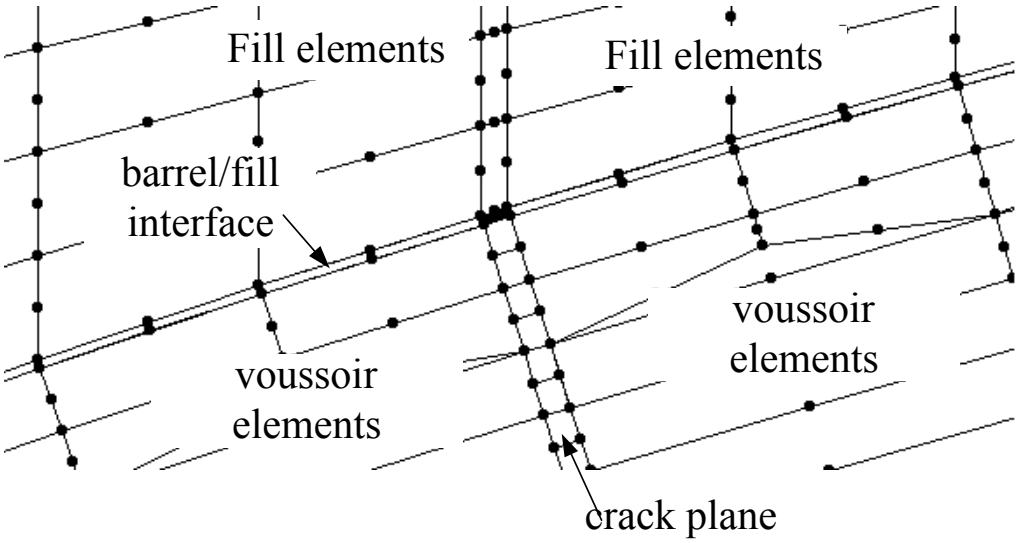

Figure 7: Modelling the interface between fill and barrel

6.2 Initial experimentation

The full mesh for the Strathmashie arch with fill for these initial experiments is shown in Figure 8. (The fill extends beyond the barrel abutments and horizontal displacement only is fixed to zero along the vertical fill boundaries). The material properties for the fill and interface are given in Table 3.

Using the same properties for the arch barrel as previously, it was not possible to form a mechanism in the bridge model with fill at imposed loads similar to the real collapse load. To form hinges at imposed loads of similar magnitude to that of the real collapse load it was found necessary to use different barrel properties. Reducing the tension cut-off T in the crack plane point contact elements to 10kN led to the

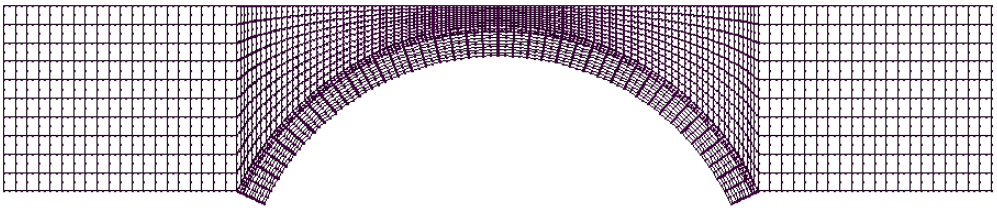

Figure 8: Initial mesh for Strathmashie Bridge with fill

formation on one hinge, on the intrados underneath the point load. Reducing *T* to 10N gave similar results. After further investigation it was concluded that the fill elements above the hinge locations were preventing hinge formation due to the fill stiffness and its inability to yield. Rather than adopt an elasto-plastic material model for the fill (which would increase the model complexity unnecessarily) the fill stiffness was varied.

Fill		**Interface**	
Young's Modulus	50 MPa	Panel Shear Modulus	50 KPa
Poisson's Ratio, ν_f	0.2	Panel Poisson's Ratio	0.2
Density	2200 kg/m^3	Panel Density	1 kg/m^3
		Point contact elements - initial stiffness	200 GN/m

Table 3: Initial properties used for fill and barrel-fill interface

Determination of Young's modulus values for soils is difficult as stiffness depends on stress history, density and water conditions [16]. However, it is clear that this model requires the use of unrealistic values of Young's modulus to function properly. Dramatically reducing the fill stiffness in the bridge model allows hinges to form but perhaps at the expense of unrealistic deformations under the loading on the running surface. The solution is to use a low stiffness material for the fill with a much stiffer surface layer representing the running surface pavement. After some experimentation this system is found to work well.

The pavement layer has a Young's modulus of 50MPa (equivalent to that of a hard clay soil [17]) while the fill between the pavement and the barrel has a Young's modulus of only 50kPa (i.e. one thousand times less than the pavement). Both materials are also modelled as near-incompressible, by using $\nu_f = 0.49$. Therefore rather than attempting to model the fill over the arch with any realism, the model uses a material formulation that produces similar behaviour, in terms of load carrying. Clearly models incorporating complex constitutive models for the fill (including yielding) are possible (indeed Reference [12] contains just such a model), and will then provide information on deformations, but at the expense of additional complexity.

7 Performance of the model with fill

7.1 Strathmashie Bridge

The properties of the model used to replicate the Strathmashie Bridge failure [1, 11] are given in Table 4

Fill		**Interface**	
Young's Modulus	50 kPa	Panel Shear Modulus	10kPa
Poisson's Ratio, ν_f	0.49	Panel Poisson's Ratio	0.2
Density	2200 kg/m^3	Panel Density	1 kg/m^3
		Point contact elements-initial Stiffness	200 GN/m
Pavement		Point contact elements-*T*	100MN
Young's Modulus	50MPa		
Poisson's Ratio	0.49		
Density	2200 kg/m^3		

Table 4: Final properties adopted for Strathmashie bridge model with fill

The point contact elements in the interface between barrel and fill are given very high tensile strength to prevent separation. The fill can, however, slide against the barrel. Removing separation but allowing sliding seems to be a reasonable model of the real interface. The mesh is shown in Figure 9 and has 7069 nodes, 1410 fill elements, and 141 pavement elements. The arch barrel is similar to the model used in Section 5.1.

As with the bare arch ring models, the crack plane properties of this model were varied until failure occurred at the correct load. The same material properties were then transferred to the model of Bridgemill Bridge. The value of *T* required to induce mechanism failure at the same load as in the real test (Appendix 1) is considerably lower than the value required in the plain arch barrel models. In the case of Strathmashie *T* = 10N.

When the Strathmashie Bridge properties were used in the Bridgemill model, with a point load of 400 kN applied, the analysis failed to converge at the load step 240-280 kN. This represents an underestimate of 34% of the real ultimate load of the bridge. To achieve failure of Bridgemill Bridge at the correct failure load, the tension cut-off for the crack planes *T* was increased to 100N.

The value of the tension cut-offs for the bridges with fill are very low in comparison to the values needed in the plain barrel analyses. The values are, however, closer to one assumption made in the Mechanism Method of zero tensile strength for the masonry in the arch barrel. Of greater interest is that, in contrast to

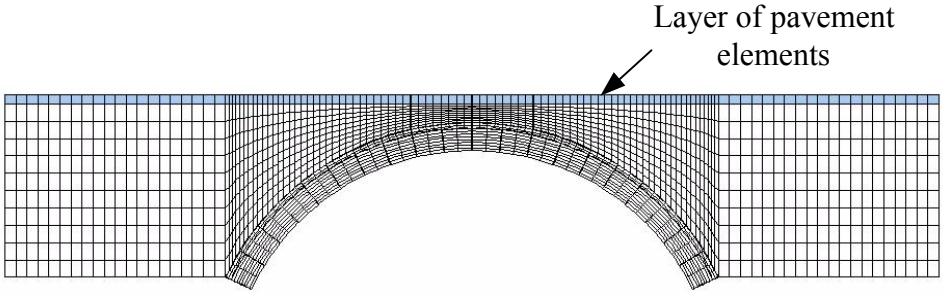

Figure 9: Final mesh for Strathmashie Bridge with fill

the barrel only analyses, *T* for Bridgemill is higher for collapse at the correct load than for Strathmashie. The different depths of fill coupled with the bridges' shapes can explain this behaviour. Strathmashie is a deep arch therefore there is more fill in contact with the arch ring for a given span, and the rate of change of fill depth away from the crown is higher. Bridgemill in contrast is a shallow arch with smaller rate of change of fill depth away from the crown. Bridgemill has one third of the fill depth at the crown of Strathmashie and so there is less dispersal of load and therefore the crack planes have to be stronger.

Practising engineers will be interested in the computer resources needed to conduct these analyses. In this study the wall clock time taken to complete a solve of a model with fill varied depending on the number of load increments and the speed of convergence, if at all, to a solution. The number of load increments was normally around 8-10 to be able to assess the failure of a bridge with adequate accuracy. Using an AMD Athlon 1800 processor, the solutions take around 6 hours.

7.1 Investigating the effect of the fill on stability

Having devised models of bridges with fill for Strathmashie and Bridgemill they were used to investigate the effect of the fill on the collapse load. The depth of the fill at the crown was varied for both Bridgemill and Strathmashie Bridges. Analyses were carried out with the actual fill depth, double and then quadruple fill depth. These were carried out with two different imposed load application positions, on the pavement above the fill at quarter span, and on the extrados of the arch ring at quarter span.

The load application position was changed to observe the effect of load dispersal through the fill on the stability of the arch. The effect was quantified by comparing displacements between load positions. Throughout the preceding discussion the simplicity of material models have been emphasised, as has the interest in loads rather than displacements. It may, therefore, seem strange to examine displacements predicted by the model, however, we are only using displacement as a relative measure between models with different fill.

Results of these analyses are shown in Figures 10-12. Surface displacements are plotted at points on the vertical axis of load application (the loaded quarter span), and at the far quarter span from the load, the remote hinge. All results are normalised with respect to the barrel thickness (for displacement) and to a load 80% of ultimate (for load). Results are given for load applied at the surface and on the barrel extrados. At the loaded quarter span the vertical displacements are plotted, as variations in displacements at this point are likely to be associated with load dispersal effects, which predominantly affect arch barrel movements in the vertical

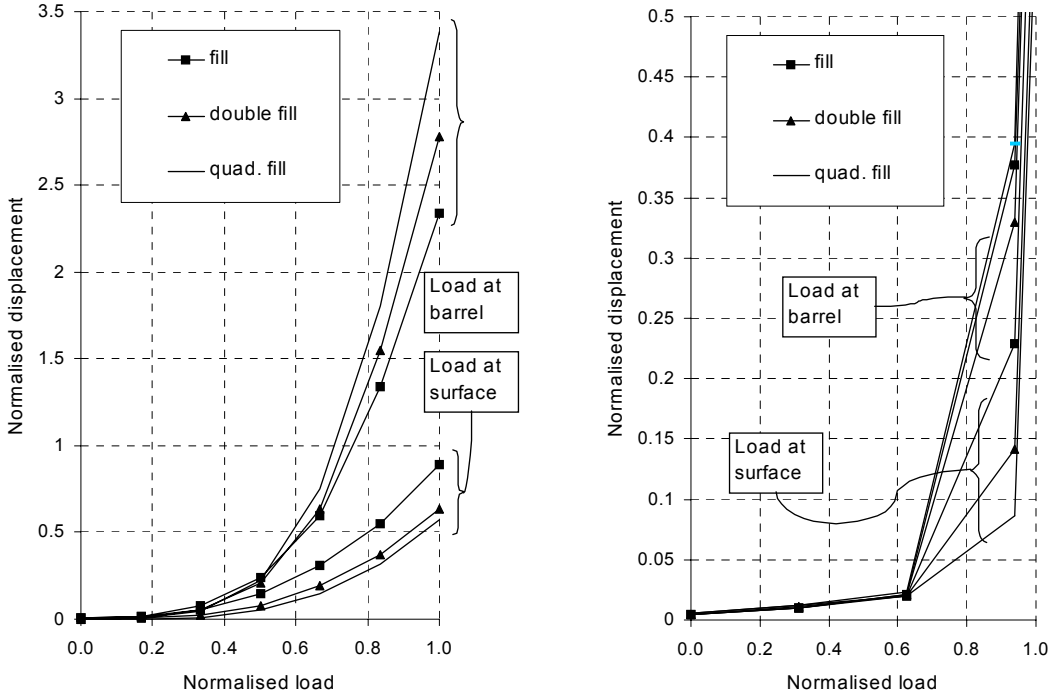

Figure 10: Vertical displacement under load, (a) Strathmashie (b) Bridgemill

plane at this location. At the remote hinge, both horizontal and vertical displacements are shown since displacements at this point on the arch barrel are influenced by the weight and passive resistance of the fill as the barrel is moving upwards at this point. The dead weight tends to restrict vertical movement and passive resistance restricts horizontal, although neither of these are mutually exclusive.

Figure 10a shows vertical displacements at the loaded quarter span for Strathmashie Bridge indicating that the smallest displacements arise with quadruple fill depth and the load applied at the surface. This is as expected, as the greater fill depth allows for more dispersal of the load so lower stress is imposed on the arch ring. Conversely, the highest displacement occurs with quadruple depth fill and load applied to the arch barrel. This demonstrates the dominant effect of load dispersal through fill.

Tests on the Bridgemill model are in a similar pattern to those for Strathmashie (Figure 10b). Bridgemill differs from Strathmashie, however, by showing less smooth variation in displacement with applied load. There is a sudden change of gradient of the curve at two-thirds of the failure load which suggests that the reduction in stiffness due to formation of hinges in the Bridgemill model is more

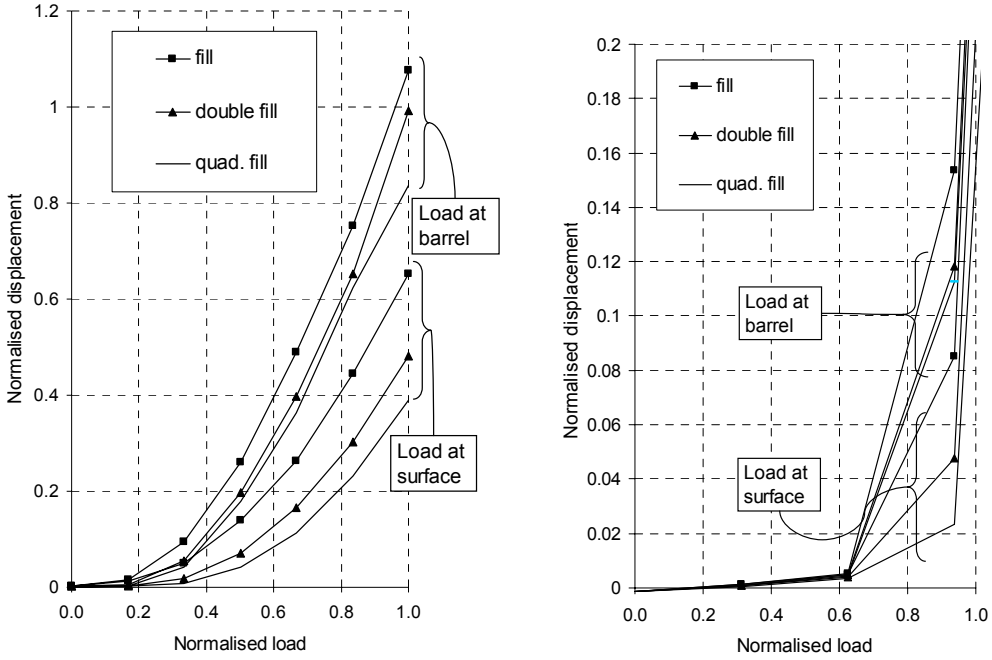

Figure 11: Horizontal displacement at remote hinge, (a) Strathmashie (b) Bridgemill

extreme than in Strathmashie. This is possibly due to the arch shape.

Table 5 shows the ratios of vertical displacement at the loaded quarter span for 300kN loading at the arch barrel against the same load at the surface.

Fill Depth	**Strathmashie**	**Bridgemill**
Normal	1.59	1.65
Double	2.66	2.32
Quadruple	4.14	4.56

Table 5: Ratios of displacements for loading at barrel against loading at surface.

While there is reasonable agreement between the ratios for Strathmashie and Bridgemill they do not follow an obvious pattern. The beneficial effect of load dispersal seems to become greater as fill is increased in the Strathmashie model while the opposite seems to happen with the Bridgemill model. So, while it is clear that increasing fill leads to greater stability, quantifying these effects using the models is difficult.

Figure 11 shows the horizontal displacements at the remote hinge location. Once again quadruple depth fill with a surface-applied load gives the lowest displacements for both models. As with the displacements under the load, Strathmashie produces a smooth, progressive curve, whereas Bridgemill has a rapid

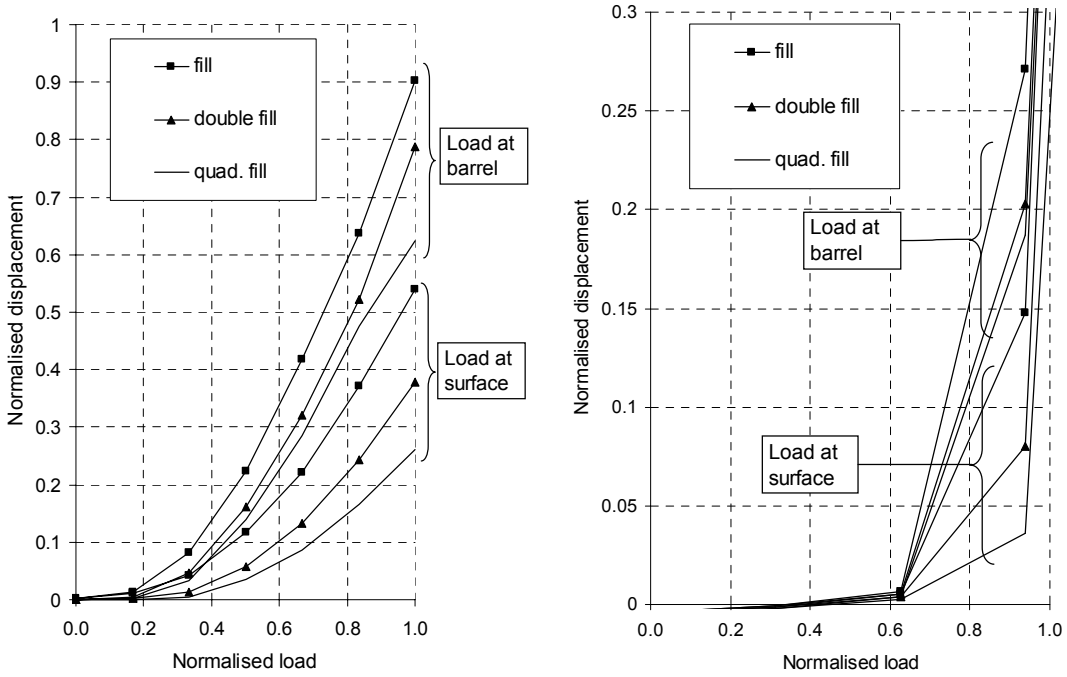

Figure 12 Vertical displacement at remote hinge, (a) Strathmashie (b) Bridgemill

change of gradient close to the two-thirds failure load mark. It is also notable that, for Bridgemill, values are small until this point indicating a sudden loss of stiffness in contrast to Strathmashie's gradual softening. There is also a spread of results at low load levels for Strathmashie, as the fill is changed and the load position moved. This is not seen in Bridgemill. The difference in behaviour could be classified as ductile and brittle respectively.

The greater depth of fill over the Strathmashie arch at the remote hinge results in higher vertical and horizontal stresses (σ_v, σ_h) in the fill at the barrel fill interface. This promotes stability during load application. In advanced soil modelling one would be interested in modelling correct values of the earth pressure coefficient at rest

$$K_0 = \frac{\sigma_h}{\sigma_v} \tag{4}$$

(taking effective stress = total stress). In this model, since elasticity is used, the K_0 values tend to $\nu/(1-\nu) \approx 1.0$ which is in the range of realistic values for soil. The increase in resistance due to mobilisation of passive pressure is not directly modelled here so one would expect the effect of fill to be more pronounced in reality than predicted by this model.

Figure 12 shows vertical displacements at the remote hinge location and again show the same pattern as for the other displacement plots. The vertical displacement is possibly affected more by fill depth leading to greater vertical stress than other factors. Bridgemill appears more affected by the increase in fill depth than Strathmashie possibly due it being a shallower arch, The vertical stress in the fill may have a greater effect in the Bridgemill model as there would be a smaller component tangential to the arch and hence less propensity to slide along the interface.

This study of varying fill depth demonstrates that the modelling used here follows expectations from empirical results. It also shows how the behaviour of the bridge as aspects of its construction are changed can be modelled. Arch bridges have been strengthened in the past by increasing the fill (or more usually the surfacing) and this model could provide a way of quantifying the stabilising effect of greater fill depth.

8 Model limitations

There are clear simplifications made in the models described above but these are justified by the desire to minimise complexity and make the techniques accessible to industry. Some of the limitations are now discussed further.

Modelling a three-dimensional structure as two-dimensional imposes certain limitations. The effects of spandrel walls cannot be included into the model, and behaviour transverse to the span cannot be observed. Although the stiffening effect associated with spandrel walls should not be included at the ultimate limit state due to their tendency to separate before failure, they still affect arch behaviour. For example, the load dispersal at the centre point of the width of the bridge will be greater than at the edge, as the spandrel wall will prevent dispersal in one direction.

Abutment movement is also totally ignored in these models. In a real structure, it is likely that abutments will not be fully rigid and will move, depending on the axial force through the arch and the passive resistance behind the abutments. As Heyman [18] has pointed out, even very small movement of abutments changes the equilibrium state of an arch dramatically. This effect is partially recognised in Pippard's analysis although it is not taken beyond assuming that abutment movement forms hinges at supports. Neglecting abutment movement and conducting a geometrically-linear analysis means snap-through behaviour cannot be modelled as this requires abutment movement.

Due to the method of crack modelling in the arch, cracks are forced to propagate perpendicular to the arch ring and at pre-defined crack planes. An improved model could include more crack planes, although experiments conducted with these models indicate very little change in behaviour in this case, for added complexity. Modelling the imposed loading as a point load leads to high and unrealistic stress concentrations in finite element analysis, although it is clearly conservative from the assessment engineer's point of view. The use of point loading with a elastic-plastic model could lead to unrealistic localised yielding

Clearly, further research is required to develop the model to gain confidence in its ability to predict collapse loads of masonry arch bridges. Despite the number of material parameters in the model, our experiments have found only one to be significant, the crack plane point contact element tensile cut-off, *T*.

9 Conclusions

A new approach has been developed for the modelling of masonry arch bridges using commercial FEA software. This semi-discrete model incorporates fill and can re-create behaviour of three bridges tested to destruction by the TRL [4]. Material properties were found from modelling one of the TRL tested bridges that were applied to models of two other bridges to predict their failure loads.

While simplistic, this model could prove useful to engineers assessing these structures who have access and familiarity with basic FEA software. The use of a mixture of finite elements, to model simple voussoirs and crack planes has been demonstrated and could be applied to any other masonry arch. The simplifications made in this modelling seem reasonable in comparison to those made in methods such as MEXE upon which most assessment work has been based to date.

Nowadays generation of two-dimensional meshes for plane strain analyses as described here is simple and usually part of the FEA software. While the non-linearities in the models do require lengthy non-linear solutions, they are not excessive on modern hardware and certainly fit in with the rule-of-thumb that dictates any computer analysis in industry must be shorter than "overnight".

10 Acknowledgements

The authors would like to thank Professor Grant Steven for help in the development of these numerical models.

11 References

[1] Page, J. "Masonry arch bridges – TRL state of the art review". HMSO, London, 1993.

[2] Hughes T. G., Blackler M. J. "A review of the UK masonry arch assessment methods", Proc. Inst. Civ. Engrs, 122, 305-315, 1997.

[3] Hughes, T.G., Hee, S.C., Soms, E. "Mechanism analysis of single span masonry arch bridges using a spreadsheet", Proc. Inst. Civ. Engrs – Structures and Buildings, 152(4), 341-350, 2002.

[4] www.obvis.com

[5] Gilbert, M., Melbourne, C. "Rigid-block analysis of masonry structures", The Structural Engineer, 72, 356-361,1994

[6] http://www.shef.ac.uk/ring/index.html

[7] Towler, K.D.S. "Applications of non-linear finite element codes to masonry arches", Proc 2nd International Conference on Civil and Structural Engineering Computing, 1985

[8] Crisfield M. A. “Finite element and mechanism methods for the analysis of masonry and brickwork arches”. Transport and Road Research Laboratory, London, 1985.
[9] Loo, Y. and Yang, Y. “Cracking and failure analysis of masonry arch bridges”, ASCE J. Struct. Eng., 117(6) 1641-1659.
[10] Choo, B.S., Coutie, M.G. and Gong, N.G. “Finite element analysis of masonry arch bridges using tapered elements”, Proc. Inst. Civ. Engs. Part 2, 91, 755-770, 1991
[11] Ng KH, Fairfield CA, Sibbald A. “Finite-element analysis of masonry arch bridges”, Proc. Inst. Civ. Engrs – Structures and Buildings 134, 119-127, 1999.
[12] Thavalingam A, Bicanic N, Robinson JI, Ponniah D.A. “Computational framework for discontinuous modelling of masonry arch bridges” Computers and Structures, 79, 1821-1830, 2001
[13] Liu, G., Houlsby, G.T. and Augarde, C.E. “Two-dimensional analysis of settlement damage to masonry buildings due to tunnelling”, *The Structural Engineer,* 79(1), January, 19-25
[14] Lee JS, Pande GN, Middleton J, Kralj B. “Numerical modelling of brick masonry panels subject to lateral loadings”, Comp. Struct., 61, 735-745, 1996
[15] Craig, R.F., “Soil Mechanics, Sixth Edition”, Spon Press, London. 1997
[16] Bowles, J.E., “Foundation analysis and design”, McGraw-Hill, Singapore. 1997
[17] Heyman, J., “The Masonry Arch”, Ellis Horwood. 1982

Appendix 1

Bridges tested under the TRL program (after [1] and [11])

Name	Approx. shape	Span (m)	Rise (m)	Barrel thickness (m)	Fill thickness at crown (m)	Experimental Collapse load per metre width (kN)
Strathmashie	Segmental	9.425	2.99	0.60	0.61	228
Bridgemill	Parabolic	10.36	2.84	0.71	0.20	373
Barlae	Segmental	9.865	1.695	0.45	0.29	296